

# Non-thermal origin of nonlinear transport across magnetically induced superconductor-metal-insulator transition

Y. Seo<sup>1,\*</sup>, Y. Qin<sup>1</sup>, C. L. Vicente<sup>1</sup>, K. S. Choi<sup>1,2</sup>, and Jongsoo Yoon<sup>1</sup>

<sup>1</sup>*Department of Physics, University of Virginia, Charlottesville, VA 22903, U.S.A.*

<sup>2</sup>*Department of Physics, Sunchon National University, Sunchon, Jeonnam, Korea.*

(Dated: October 31, 2018)

We have studied the effect of perpendicular magnetic fields and temperatures on the nonlinear electronic transport in amorphous Ta superconducting thin films. The films exhibit a magnetic field induced metallic behavior intervening the superconductor-insulator transition in the zero temperature limit. We show that the nonlinear transport in the superconducting and metallic phase is of non-thermal origin and accompanies an extraordinarily long voltage response time.

In recent years, the suppression of superconductivity in two-dimensions (2D) by means of increasing disorder (usually controlled by film thickness) or applying magnetic fields has been a focus of attention. Conventional treatments [1, 2, 3, 4, 5] of electronic transport predict that in 2D the suppression of the superconductivity leads to a direct superconductor-insulator transition (SIT) in the limit of zero temperature ( $T = 0$ ). This traditional view has been challenged by the observation of magnetic field ( $B$ ) induced metallic behavior in amorphous MoGe [6, 7, 8] and Ta thin films [9]. The unexpected metallic behavior, intervening the  $B$ -driven SIT, is characterized by a drop in resistance ( $\rho$ ) followed by a saturation to a finite value as  $T \rightarrow 0$ . The metallic resistance can be orders of magnitude smaller than the normal state resistance ( $\rho_n$ ) implying that the metallic state exists as a separate phase rather than a point in the phase diagram. Despite many theoretical treatments [8, 10, 11, 12, 13, 14, 15, 16, 17], a consensus on the mechanism behind the metallic behavior is yet to be reached. Proposed origins of the metallic behavior include bosonic interactions in the non-superconducting phase[10, 11], contribution of fermionic quasiparticles to the conduction[12, 13], and quantum phase fluctuations[14, 15].

In a recent paper [9] on the magnetically induced metallic behavior in Ta films, we have reported the nonlinear voltage-current ( $I$ - $V$ ) characteristics that can be used to identify each phase. The superconducting phase is unique in having both a hysteretic  $I$ - $V$  and an “immeasurably” small voltage response to currents below an apparent critical current  $I_c$ . The metallic phase can be identified by a differential resistance ( $dV/dI$ ) that increases with increasing  $I$ , whereas the insulating phase is identified by a  $dV/dI$  that decreases with increasing  $I$ . The contrasting nonlinear  $I$ - $V$  in the metallic and insulating phase are shown in Fig. 1(a).

The main purpose of this Letter is to report that the origin of the nonlinear transport, particularly in the superconducting and metallic phase, is not a simple reflection of  $T$ -dependence of  $\rho$  via the unavoidable Joule heating. We describe the effect of  $B$  and  $T$  on the nonlinear

TABLE I: List of sample parameters: nominal film thickness, mean field  $T_c$  at  $B = 0$ , normal state resistivity at 4.2 K, critical magnetic field at which the resistance reaches 90% of the high field saturation value, and correlation length calculated from  $\xi = \sqrt{\Phi_0/2\pi B_c}$  where  $\Phi_0$  is the flux quantum.

sample	batch	$t(nm)$	$T_c(K)$	$\rho_n(\Omega/\square)$	$B_c$	$\xi$
Ta 1	1	3.5	0.584	1769	0.72	21
Ta 2	1	5.0	0.675	1180	0.88	19
Ta 3	2	5.7	0.770	1056	0.9	19
Ta 4	3	5.0	0.598	770	-	-
Ta 5	4	36	0.995	69	2.0	13

transport on which this conclusion is based. We also present our studies on dynamic voltage response which reveal strikingly long voltage response times that accompany the nonlinear transport.

Our samples are dc sputter deposited Ta thin films on Si substrates. The sputter chamber is baked at  $\sim 110^\circ\text{C}$  for several days, reaching a base pressure of 10-8 Torr. The chamber and Ta source were cleaned by pre-sputtering for  $\sim 30$  min at a rate of  $\sim 1\text{nm/s}$ . Films are grown at a rate of  $\sim 0.05\text{ nm/s}$  at an Ar pressure of  $\sim 4\text{ mTorr}$ . Using a rotatable substrate holder up to 12 films, each with a different thickness, can be grown without breaking the vacuum. In order to facilitate four point measurements, the samples are patterned into a bridge (1 mm wide and 5 mm long) using a shadow mask. Even though there were noticeable batch to batch variations, the degree of disorder (evidenced by the values of  $\rho_n$ ) for films of the same batch increases monotonically with decreasing film thickness. The superconducting properties of the films are characteristic of homogeneously disordered thin films [18], and consistent with the results of x-ray structural investigations [9]. The data presented in this paper are from 5 films grown in 4 batches. Parameters of the films are summarized in Table I.

The evolution of the  $I$ - $V$  curves across the superconductor-metal boundary at 40 mK is shown in Fig. 1(b) for sample Ta 1. The hysteretic  $I$ - $V$ , unique to the superconducting phase, is indicated by the dashed lines. As  $I$  is increased, the superconductivity is abruptly

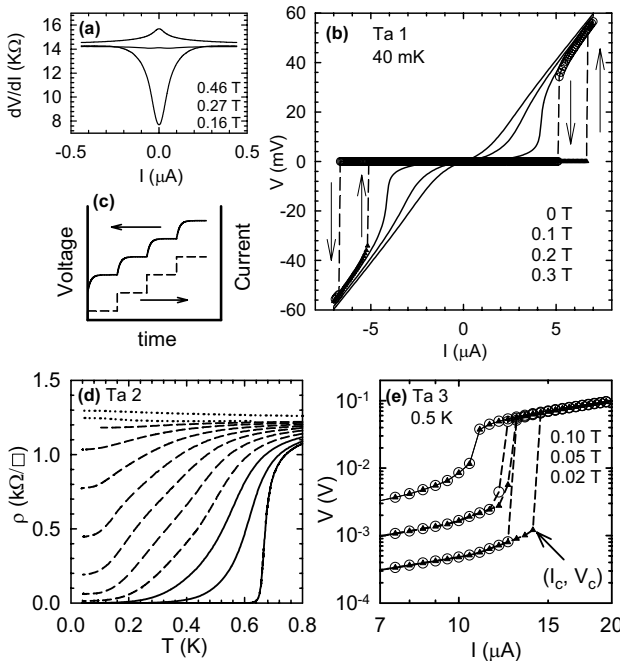


FIG. 1: (a)  $dV/dI$  vs.  $I$  at 20 mK across the metal-insulator boundary for a Ta film with  $T_c = 0.23$  K, adapted from Ref.[9]. (b) Current biased I-V curves of sample Ta 1 at 40 mK and the indicated  $B$ . (c) Our method of  $I$ - $V$  measurements is illustrated. (d) The  $T$ -dependence of  $\rho$  for sample Ta 2 at  $B = 0 - 1.0$  T with 0.1 T interval and 3.0 T, measured at 7 Hz with a current amplitude of 1 nA. The solid lines are to indicate the superconducting phase in the low  $T$  limit, the dashed lines the metallic phase, and the dotted lines insulating phase. (e) I-V curves in log-log scale for sample Ta 3. Filled triangles (open circles) are for current increasing (decreasing) branch. The data density is reduced to make individual symbols visible. The arrow marks the critical current  $I_c$  and voltage  $V_c$ .

quenched at a well-defined critical current  $I_c$ . As  $I$  is decreased from above  $I_c$ , the superconductivity suddenly appears at a different current  $I'_c < I_c$ . The hysteresis becomes smaller with increasing  $B$ , and vanishes near 0.1 T as the system is driven into the metallic phase [solid lines in Fig. 1(b)]. Typical  $T$ -dependence of  $\rho$  at various  $B$  is shown in Fig. 1(d) for another sample Ta 2. In this sample, which is less disordered than Ta 1, the superconducting phase extends up to  $\sim 0.2$  T [solid lines in Fig. 1(d)] and the metallic behavior is observed at higher  $B$  up to  $\sim 0.9$  T (dashed lines). Hereafter, “superconducting regime” refers to the transport regime where I-V is hysteretic and “metallic regime” to the regime with nonlinear (and reversible) I-V with increasing  $dV/dI$  with increasing  $I$ .

All our I-V curves are constructed by plotting the steady state voltage at each bias current that is changed in small discrete steps as illustrated in Fig. 1(c). In order to ensure that the steady state is reached at each step, the voltage is monitored every 50 ms for up to 55 s while the current is kept constant. The magnitude of

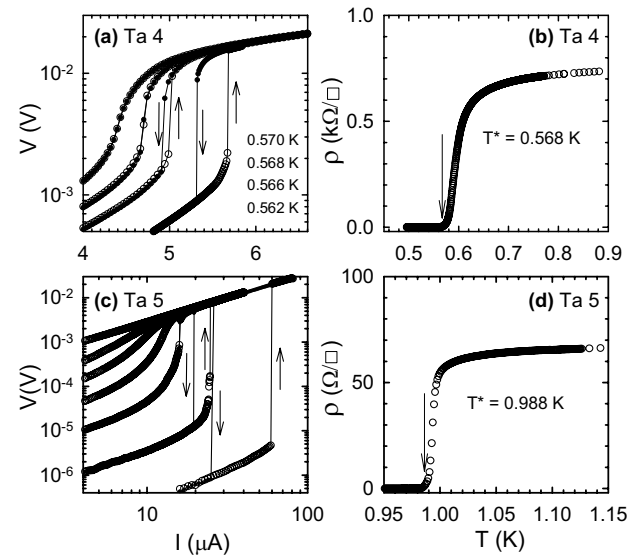


FIG. 2: (a)  $I$ - $V$  curves of sample Ta 4 at  $B = 0$  and at the indicated  $T$ . Open (filled) circles are for the current increasing (decreasing) branch. (b)  $T$ -dependence of  $\rho$  for sample Ta 4 at  $B = 0$ . The arrow is to indicate the temperature  $T^*$  where the hysteresis vanishes. (c) The  $I$ - $V$  of the sample Ta 5 at  $B = 0$ . The temperature of each trace is, from the top, 1.000, 0.994, 0.992, 0.990, 0.988, 0.984, and 0.976 K. (d) The  $T$ -dependence of  $\rho$  for sample Ta 5 at  $B = 0$ .

the voltage jump at  $I_c$  (or  $I'_c$ ), which could be as large as several orders of magnitude, was almost independent of the current step size in the range 5 - 100 nA. Even with our smallest steps of 5 nA, no steady state with a voltage within the range covered by the jump was observed.

Our investigations on how  $B$  and  $T$  influence the nonlinear transport indicate that these quantities play similar roles. The main effect of increasing  $T$  is to lower the superconductor-metal “critical” field  $B_c^{sm}$ ; the  $B$ -driven evolution of the I-V curves at an elevated  $T$  [Fig. 1(e)] remains qualitatively the same as that in the low  $T$  limit [Fig. 1(b)]. More importantly, the evolution of the I-V curves as a function of  $T$  [shown in Fig. 2(a) and (c)] is strikingly similar to that caused by  $B$  [shown in Fig. 1(b) and (e)].

The field  $B_c^{sm}$  decreases with increasing  $T$  and reaches zero at a well-defined temperature  $T^*$ , which is close to  $T_c$  as shown by the arrows in Fig. 2(b) and (d). This, together with the observations described above, means that  $B_c^{sm}$  is a well-defined line in  $B$ - $T$  plane separating the superconducting and metallic regime. We point out that, in terms of nonlinear transport, the electronic properties at  $B \gtrsim B_c^{sm}$  in the low  $T$  limit, where the unexpected metallic behavior intervening SIT is observed, are indistinguishable from those at high temperatures, for example at  $T \gtrsim T^*$  and  $B \approx 0$ .

An important finding from our investigations is that the voltage jump in the superconducting regime is of

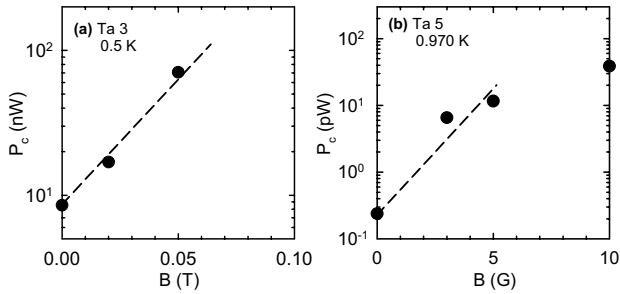


FIG. 3: (a) The  $B$ -dependence of the critical power,  $P_c = I_c V_c$ , for sample Ta 3 at 0.5 K.  $I_c$  and  $V_c$  are marked by an arrow in Fig. 1(e). The dashed line is to guide an eye. (b)  $P_c$  vs.  $B$  plot for sample Ta 5 at 0.970 K.

non-thermal origin. If Joule heating is significant, the electron temperature  $T_e$  would be determined by the balance of the Joule heating power and the heat drain rate to the stage where the sample is thermally anchored. A large heating power at a high bias current could make  $T_e$  substantially higher than the stage temperature. If  $T_e$  reaches near  $T_c$  where  $\rho$  sharply rises with  $T$ , an increase in  $T_e$  could cause an increase in the heating power, which in turn causes a further increase in  $T_e$ . Such a positive self-feedback would make  $T_e$  unstable and run away beyond  $T_c$ , resulting in a sudden quenching of the superconductivity appearing as a voltage jump. This scenario can be tested by applying weak  $B$ . The magnetic fields lower  $T_c$  while the net thermal conductance between the sample and the stage would remain almost unaffected. Therefore, in the heating scenario the critical power,  $P_c = I_c V_c$  where  $I_c$  and  $V_c$  are the current and voltage at the onset of the voltage jump on the current increasing branch [marked by an arrow in Fig. 1(e)], is expected to be weakly decreasing function of  $B$ . However, as shown in Fig. 3(a) and (b),  $P_c$  is found to increase by an order of magnitude or more under weak  $B$ . This clearly demonstrates that the voltage jump in the superconducting regime has a non-thermal origin. We note that  $V_c$  is the highest steady state voltage in the superconducting state before the current-induced sudden quenching of the superconductivity. In repeated runs after thermal cyclings to above 10 K, the value of  $V_c$  was reproducible within several percent even with different current step sizes in the range 5 - 100 nA.

The  $I$ - $V$  curves in Fig. 1-2 clearly show that the discontinuity in  $I$ - $V$  in the superconducting regime evolves into the point of the largest slope in the continuous  $I$ - $V$  in the metallic regime. This strongly suggests that the sudden quenching of the superconductivity at  $I_c$  and the nonlinear transport in the metallic regime are caused by the same mechanism, which has been shown above to be of non-thermal origin.

Now we turn to the discussion on the dynamic voltage response. The dynamic voltage response was studied by

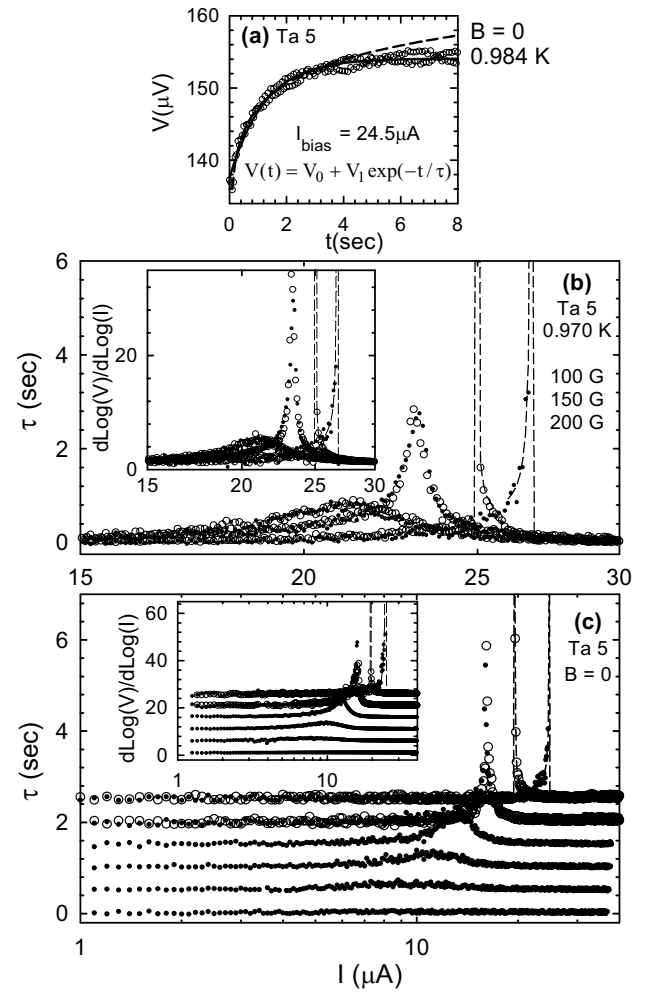


FIG. 4: (a) An example of  $V$ - $t$  trace at  $I = 24.5$  A. The solid line is a fit to the exponential function shown. The dashed line is a fit to a logarithmic  $t$ -dependence for the first 3 s. (b)  $t$  vs.  $I$  plot at the indicated  $B$  and  $T$ . Filled (open) circles are for current increasing (decreasing) branch. The dashed lines are to guide an eye. Inset: the slope of  $I$ - $V$  curves in log-log scale at the same  $B$  and  $T$ . (c)  $\tau$ - $I$  plot at  $B = 0$ . The temperature of each trace is, from the top, 0.984, 0.988, 0.990, 0.992, 0.994, and 1.000 K. Each trace is vertically shifted successively. For the bottom four traces, only current increasing branch is shown. Inset:  $d(\log V)/d(\log I)$  is plotted at the same  $T$  and  $B$ . Each trace is vertically shifted successively.

analyzing the voltage-time ( $V$ - $t$ ) traces to determine how fast the steady state is reached at each bias current. As shown by the solid line in Fig. 4(a), the  $t$ -dependence is well described by an exponential function. The parameters  $V_0$  and  $V_1$  are determined from the measured steady state voltage and  $V(t = 0)$  which is the steady state voltage at the previous bias current. The parameter  $\tau$  is defined as the voltage response time constant, and obtained from a least squared error fitting procedure.

Figure 4(b) shows the  $\tau$ - $I$  plots at three different  $B$  across the superconductor-metal boundary. In the su-

superconducting regime ( $B=100$  G), the time constant exhibits a hysteretic and diverging behavior with approaching  $I_c$  from below ( $I'_c$  from above) where the  $I$ - $V$  is discontinuous. In the metallic regime (150 and 200 G) where  $I$ - $V$  is continuous and reversible, the  $\tau$ -traces are also continuous and reversible. However, a prominent peak structure is evident in the data. Interestingly, the peak or diverging feature in  $\tau$  almost exactly coincides with the nonlinear transport. The inset shows the slopes of  $I$ - $V$  curves in log-log scale. At current where  $\tau$  is large the transport is nonlinear [ $d(\log V)/d(\log I) > 1$ ], and at current where  $\tau$  is almost zero the transport is linear [ $d(\log V)/d(\log I) = 1$ ]. Qualitatively the same  $\tau$  behavior is observed when the superconductor-metal boundary is crossed by increasing  $T$ . This is shown in Fig. 4(c). Note that the traces in Fig. 4(c) and the inset are successively shifted vertically.

It is surprising to find that the time constant in the peak or diverging region is as long as several seconds. We emphasize that the long time constant is not due to instrumentation. This is best demonstrated by the systematics of the data. Changing  $B$  or  $T$  systematically shifts the peak or divergence while outside the narrow peak or diverging region the time constants remain almost zero. The time constants were measured to be the same within the scatter of the data for current steps of 5 nA (not shown) and 100 nA (shown).

In the past, hysteresis accompanying a long response time has been studied in the context of irreversible magnetic properties in type II superconductors [19]. Large magnetic relaxation rates observed in magnetization measurements [20] are believed to arise from thermal activation of magnetic flux lines out of pinning sites. The depinning process leads to a redistribution of flux lines causing a change in magnetization with time. Although our hysteresis with a long response time is observed in transport, not magnetization measurements, it still may be possible to understand in terms of pinning-depinning of vortices. A pinning-depinning transition arises from the competition between disorder-induced pinning force and Lorentz driving force due to the bias current. Under such a competition, the vortex motion is analogous to the flow of sand grains in a sand pile [21], where the competition is between the jamming due to the granularity of the system and gravitational force. Indeed, hysteresis [22] and slow relaxation rates [23] have been observed in granular flow under mechanical vibrations. Logarithmic time dependence has been observed in measurements of relaxation of magnetization [19] and experiments on granular flow[23]. The dashed line in Fig. 4(a) is the fit of our data to a logarithmic time dependence, and describes the data well for  $t < 3$  s. Nevertheless, over the entire range of the data, the exponential function (solid line) fits our data better.

Finally, we briefly discuss an interesting implication of the unusually long response time accompanying the

nonlinear transport at  $B = 0$  and  $T \gtrsim T^*$ . Nonlinear transport of 2D superconductors at  $B = 0$  is usually understood in the framework of Kosterlitz-Thouless (KT) theory [24], where the superconducting transition corresponds to a thermodynamic instability of vortex-antivortex pairs in 2D. In this picture, current-induced dissociation of vortex pairs in the superconducting phase is expected to lead to nonlinear transport in the fashion,  $V \propto I^a$  with  $a > 3$  [25]. It has been argued [26] that in a real system finite size effect can induce free vortices altering the power law  $I$ - $V$ . The resulting  $I$ - $V$  curves obtained in numerical simulations [26] show a pronounced peak structure in  $d(\log V)/d(\log I)$  resembling those shown in the inset of Fig. 4(c). However, the voltage response time which is observed to be as long as several seconds, is too long to be reasonable with the KT framework where the vortex dissociation is expected to occur in the time scale of quasiparticle scattering, typically  $\sim 10^{-9}$  s [27]. At present, whether dynamics of KT vortices in the presence of disorder can have such long time scales is not clear, and the understanding of the nonlinear transport requires the development of a theoretical framework for nonequilibrium dynamics.

In summary, we have shown the magnetic field and temperature driven evolution of phase-identifying nonlinear  $I$ - $V$  characteristics of Ta thin films that exhibit an unexpected metallic phase intervening SIT in the low  $T$  limit. Our observations indicate that a non-thermal mechanism is behind both the nonlinear transport in the metallic phase and sudden current-induced quenching of the superconductivity in the superconducting phase. Our dynamic voltage response studies suggest a possible link of the metallic behavior to the dynamics of vortices in the presence of disorder.

Authors acknowledge fruitful discussions with V. Galitski, H. Fertig, and E. Kolomeisky. This work is supported by NSF.

---

\* Present address: Nano Science and Technology, Sejong University, Seoul, Korea.

- [1] E. Abrahams, P. W. Anderson, D. C. Licciardello, and T. V. Ramakrishnan, Phys. Rev. Lett. **42**, 673 (1979).
- [2] A. Finkelstein, JETP Lett. **45**, 46 (1987).
- [3] A. Larkin, Ann. Phys. (Leipzig) **8**, 785 (1999).
- [4] M. P. A. Fisher, Phys. Rev. Lett. **65**, 923 (1990).
- [5] M. P. A. Fisher, G. Grinstein, and S. M. Girvin, Phys. Rev. Lett. **64**, 587 (1990).
- [6] N. Mason and A. Kapitulnik, Phys. Rev. Lett. **82**, 5371 (1999).
- [7] N. Mason and A. Kapitulnik, Phys. Rev. B **65**, 220505(R) (2002).
- [8] D. Ephron, A. Yazdani, A. Kapitulnik, and M. R. Beasley, Phys. Rev. Lett. **76**, 1529 (1996).
- [9] Y. Qin, C. L. Vicente, and J. Yoon, Phys. Rev. B **73**, 100505(R) (2006).

- [10] D. Dalidovich and P. Phillips, Phys. Rev. B **64**, 052507 (2001).
- [11] D. Dalidovich and P. Phillips, Phys. Rev. Lett **89**, 027001 (2002).
- [12] V. M. Galitski, G. Refael, M. P. A. Fisher, and T. Senthil, Phys. Rev. Lett **95**, 077002 (2005).
- [13] A. Kapitulnik, N. Mason, S. A. Kivelson, and S. Chakravarty, Phys. Rev. B **63**, 125322 (2001).
- [14] D. Das and S. Doniach, Phys. Rev. B **64**, 134511 (2001).
- [15] B. Spivak, A. Zyuzin, and M. Hruska, Phys. Rev. B **64**, 132502 (2001).
- [16] S. Tewari, Phys. Rev. B **69**, 014512 (2004).
- [17] T. K. Ng and D. K. Lee, Phys. Rev. B **64**, 144509 (2001).
- [18] A. M. Goldman and N. Markovic, Phys. Today **49**, 39 (1998).
- [19] Y. Yeshurun, A. P. Malozemoff, and A. Shaulov, Rev. Mod. Phys. **68**, 911 (1996).
- [20] M. R. Beasley, R. Labusch, and W. W. Webb, Phys. Rev. **181**, 682 (1969).
- [21] S. Pla and F. Nori, Phys. Rev. Lett **67**, 919 (1991).
- [22] S. G. K. Tennakoon, L. Kondic, and R. P. Behringer, Europhys. Lett. **45**, 470 (1999).
- [23] H. M. Jaeger, C.-H. Liu, and S. Nagel, Europhys. Lett. **62**, 40 (1988).
- [24] J. D. Kosterlitz and D. J. Thouless, J. Phys. C **6**, 1181 (1973).
- [25] B. I. Halperin and D. R. Nelson, J. Low Temp. Phys **36**, 599 (1979).
- [26] K. Medvedyeva, B. Kim, and P. Minnhagen, Phys. Rev. B **62**, 14531 (2000).
- [27] B. J. Ruck, H. J. Trodahl, J. C. Abele, and M. J. Geselbracht, Phys. Rev. B **62**, 12468 (2000).